

A Determination of the Radio-Planetary Frame Tie From Comparison of Earth Orientation Parameters

M. H. Finger¹ and W. M. Folkner
Tracking Systems and Applications Section

The orientation of the reference frame of radio source catalogs relative to that of planetary ephemerides, or "frame tie," can be a major systematic error source for interplanetary spacecraft orbit determination. This work presents a method of determining the radio-planetary frame tie from a comparison of very long baseline interferometry (VLBI) and lunar laser ranging (LLR) station coordinate and Earth orientation parameter estimates. A frame tie result is presented with an accuracy of 25 nrad.

I. Introduction

Very long baseline interferometry (VLBI) offers interplanetary spacecraft navigation a highly accurate data type for orbit determination. The most commonly used data type, delta differential one-way ranging (Δ DOR), provides 50-nrad (or better) information about the angular position of a spacecraft relative to a nearby radio source [1]. The positions of radio sources within the inertial reference frame defined by extragalactic radio sources are typically known to 3–5 nrad [2]. The planetary ephemeris defines a separate inertial reference frame [3]. Knowledge of the relative global rotation, or frame tie, between these two inertial reference frames is necessary to take full advantage of VLBI tracking of interplanetary spacecraft. The uncertainty in the frame-tie calibration can be the dominant orbit determination error for inner planet approach navigation [4].

In addition to providing a navigational data type, VLBI plays another important role in spacecraft orbit determination. VLBI radio source observations are used to monitor, with 10-nrad accuracy, the orientation of the Earth with respect to inertial space. The time dependent transformation from terrestrial to celestial coordinates is expressed in terms of universal time and polar motion (UTPM) parameters and precession and nutation corrections that result from fitting the VLBI data. Since these observations refer the orientation of Earth to the radio reference frame, the radio-planetary frame tie will affect interplanetary orbit determination even when no VLBI observations of the spacecraft are employed.

Lunar laser ranging (LLR) is an alternate technique for monitoring the orientation of the Earth with respect to inertial space. The LLR observations refer the orientation of the Earth to the lunar ephemeris, which gives LLR tracking station locations in the lunar ephemeris frame. Through the effect of solar perturbations on the lunar or-

¹ Now with Astronomy Programs, Computer Sciences Corporation.

bit, the LLR data are sensitive to the ecliptic plane and the direction to the sun. The orientation of the planetary ephemeris system, as defined by the Earth's orbit, can therefore be tied to the lunar ephemeris system with about 10-nrad accuracy [3].

Since both LLR and VLBI measure the orientation of the Earth with 10-nrad accuracy, it should be possible to determine the frame tie from a comparison of these measurements. An earlier attempt to do this by Niell² was limited by a restricted ability to determine the orientation of the terrestrial frames for VLBI and LLR. Now that there are three well-determined LLR station locations, and because of recent efforts to unify terrestrial coordinate systems [5], it is possible to determine the frame tie with 15–25 nrad accuracy from a comparison of LLR and VLBI Earth orientation series.

The theoretical foundation for this comparison is established in Sections II and III. Section II examines in detail the nature of the time dependent terrestrial-celestial ties mentioned above. In Section III an expression is derived for the radio-planetary frame tie in terms of the LLR to VLBI station-coordinate system tie and the parameters of the two terrestrial-celestial ties. The LLR and VLBI solutions compared in this analysis are presented in sections IV and V, respectively.

In Section VI, a determination of the LLR to VLBI station coordinate transformation is presented. Since the VLBI stations and LLR sites are widely separated, it is necessary to use other data to bridge the two coordinate systems. A recent Crustal Dynamics Project (CDP) VLBI station location set, which includes mobile VLBI observations at LLR sites, is used to connect the LLR and VLBI terrestrial coordinate systems.

With this terrestrial tie determined, the planetary ephemeris to radio source catalog frame tie can be determined from an intercomparison of the VLBI and LLR nutation and Earth orientation parameters. This comparison and the resulting frame tie are presented in Section VII. The derived frame tie is compared with other available results in Section VIII. Some comments on how to best use the results of this work for spacecraft navigation are included in Section IX.

Much of this work parallels the current efforts of the International Earth Rotation Service (IERS). IERS is in the process of comparing and unifying terrestrial VLBI, LLR, and satellite laser ranging (SLR) coordinate systems and unifying different VLBI celestial coordinate systems with the goal of testing the consistency of various Earth rotation parameter series [6–8]. Where possible, the notation used here is consistent with that of the IERS.

II. Ties Between Celestial and Terrestrial Frames

In the process of reducing LLR or VLBI data, a time dependent transformation between implicitly defined celestial and terrestrial coordinate systems is established. This transformation represents a dynamic tie between Earth-fixed and inertial frames and includes estimated and assumed precession, nutation, and Earth orientation parameters. To employ this transformation, it must be understood in some detail. To this end, the standard representation of the orientation of the Earth with respect to inertial space is presented here. Particular attention is paid to the quantities that are commonly estimated and how they affect this representation.

Let \vec{X} represent the Earth-fixed coordinate vector of a station in an equatorial coordinate system with the x -axis nominally aligned with the Greenwich meridian.³ The station's instantaneous (J2000) celestial coordinate vector \vec{C} at time t is calculated as

$$\vec{C} = \mathbf{P} \mathbf{N} \mathbf{S} \mathbf{O} \vec{X} \quad (1)$$

The (polar motion) rotation \mathbf{O} corrects for the offset between the Earth-fixed coordinate pole and the Celestial Ephemeris Pole (CEP). The CEP is conceptually defined as the axis which, in the theory of the rotation of the Earth, has no forced daily or semi-daily nutations [9,10]. \mathbf{S} models the rotation of the Earth about the CEP, \mathbf{N} accounts for the quasi-periodic nutation of the CEP about the "mean pole of date," and \mathbf{P} models the precession, or secular drift, of the "mean pole of date" and "mean equinox of date" with respect to the celestial fixed pole and equinox of J2000. Each of these rotations is discussed in detail below.

All together, eight or more angles are used to describe the rotation between terrestrial and celestial coordinates

² A. E. Niell, "Absolute Geocentric DSN Station Locations and the Radio-Planetary Frame Tie," JPL Interoffice Memorandum 335.2-159 (internal document), Jet Propulsion Laboratory, Pasadena, California, March 21, 1984.

³ The time dependence of the Earth-fixed location due to plate motion is ignored throughout this section.

(including three precession angles, two nutation angles, two polar motion angles, and UT1-UTC). The conceptual definitions of these angles are largely a product of the historical development of the theory of the Earth's rotation. While the overall rotation can be experimentally determined, many of the intermediate rotation angles have no precise empirical definition, and thus cannot be uniquely measured. The philosophy that will be adopted here is that in the final analysis, only the total rotation matrix has a well-defined physical meaning.

A. Notation

In order to discuss modeling of Earth's rotation in detail, a notation for positive rotations \mathbf{R}_X , \mathbf{R}_Y , and \mathbf{R}_Z about the x -, y -, and z -axis, respectively, is introduced, where \mathbf{R}_X , \mathbf{R}_Y , and \mathbf{R}_Z are defined by

$$\begin{aligned}\mathbf{R}_X(\theta) &= \begin{pmatrix} 1 & 0 & 0 \\ 0 & \cos \theta & \sin \theta \\ 0 & -\sin \theta & \cos \theta \end{pmatrix} \\ \mathbf{R}_Y(\theta) &= \begin{pmatrix} \cos \theta & 0 & -\sin \theta \\ 0 & 1 & 0 \\ \sin \theta & 0 & \cos \theta \end{pmatrix} \\ \mathbf{R}_Z(\theta) &= \begin{pmatrix} \cos \theta & \sin \theta & 0 \\ -\sin \theta & \cos \theta & 0 \\ 0 & 0 & 1 \end{pmatrix}\end{aligned}\quad (2)$$

These rotations are positive in the sense that they represent a transformation between two coordinate systems with the final coordinate system's basis vectors being rotated from the initial system's basis vectors by a right-handed rotation of angle θ about the designated axis.

A rotation about an arbitrary axis will be defined by

$$\mathbf{R}(\vec{\theta})\vec{r} = \vec{r} - \sin \theta \hat{\theta} \times \vec{r} + (1 - \cos \theta)\hat{\theta} \times (\hat{\theta} \times \vec{r}) \quad (3)$$

where $\theta = |\vec{\theta}|$ is the angle of rotation, $\hat{\theta} = \vec{\theta}/\theta$ is the rotation axis, and \vec{r} is an arbitrary coordinate vector. For example, with this notation $\mathbf{R}_X(\theta) = \mathbf{R}(\theta\hat{e}_X)$, $\mathbf{R}_Y(\theta) = \mathbf{R}(\theta\hat{e}_Y)$, and $\mathbf{R}_Z(\theta) = \mathbf{R}(\theta\hat{e}_Z)$, where \hat{e}_X , \hat{e}_Y , and \hat{e}_Z are the x -, y -, and z -unit vectors, respectively. Two results will prove useful in connection with this notation. First, if \mathbf{M} is a rotation matrix, then it can be shown that

$$\mathbf{M}\mathbf{R}(\vec{\theta})\mathbf{M}^{-1} = \mathbf{R}(\mathbf{M}\vec{\theta}) \quad (4)$$

Equation (4) follows from Eq. (3) and the invariance of the cross product under orthonormal coordinate transformations ($\mathbf{M}[\vec{A} \times \vec{B}] = [\mathbf{M}\vec{A}] \times [\mathbf{M}\vec{B}]$). A second result is the approximation rule for small rotation vectors,

$$\mathbf{R}(\vec{B})\mathbf{R}(\vec{A}) \approx \mathbf{R}(\vec{A} + \vec{B} + \vec{A} \times \vec{B}/2) \quad (5)$$

which is accurate through second order.

B. Terrestrial Pole Orientation

The first rotation applied in the transformation from terrestrial to celestial coordinates is the orientation matrix \mathbf{O} , which accounts for polar motion, the offset of the CEP from the terrestrial coordinate system pole

$$\mathbf{O}(t) = \mathbf{R}\left(\begin{pmatrix} y \\ x \\ 0 \end{pmatrix}\right) \quad (6)$$

The angles x and $-y$ are approximately the x and y coordinates of the CEP in the Earth-fixed system.

C. Rotation About the Pole

The vast majority of the rotational velocity of the Earth is modeled in the spin matrix

$$\mathbf{S}(t) = \mathbf{R}_Z(-\theta_G) \quad (7)$$

where θ_G represents Greenwich Mean Sidereal Time, the hour angle between the meridian containing both the terrestrial x -axis and the CEP and the meridian containing both this pole and the mean equinox of date. The equation of the equinoxes, which is normally included with the spin rotation \mathbf{S} , will be incorporated below in the nutation matrix \mathbf{N} . It should be noted that small rotational velocities occur due to precession, nutation, and polar motion, and therefore the CEP is not the rotation axis of the Earth's crust. By definition, the Earth-rotation-based time scale UT1 is directly related to θ_G , with the explicit relationship given by [11]. When UT1 is estimated, the spin matrix may be represented as

$$\mathbf{S}(t) = \mathbf{S}_0(t)\mathbf{R}_Z(-\Omega[\text{UT1} - \text{UTC}]) \quad (8)$$

where Ω is the mean rotation rate of the Earth and $\mathbf{S}_0(t)$ is the value of $\mathbf{S}(t)$ obtained by assuming UT1 = UTC.

D. Nutation

Nutation describes the short-term quasi-periodic variations in the CEP. The longest period terms have an 18.6-year period with an amplitude of 43 μrad . The standard model for nutation is given by

$$\mathbf{N}(t) = \mathbf{R}_X(-\epsilon)\mathbf{R}_Z(\Delta\psi)\mathbf{R}_X(\epsilon + \Delta\epsilon)\mathbf{R}_Z(-\alpha_E) \quad (9)$$

where $\Delta\psi$ is the nutation in the ecliptic longitude of the pole, and $\Delta\epsilon$ is its nutation in obliquity (the angle from the ecliptic pole). Here, the equation of the equinoxes

$$\alpha_E = \Delta\psi \cos(\epsilon + \Delta\epsilon) \quad (10)$$

has been included with the nutation since the equation of the equinoxes depends only on nutation parameters. Fourier series for $\Delta\psi$ and $\Delta\epsilon$ for the standard (IAU 1980) model are given by Wahr [12] or Seidelmann [9].

To provide a better understanding of the nutation matrix, an approximate formula for it will be derived using Eqs. (4) and (5). First, using Eq. (5), the nutations can be grouped together:

$$\mathbf{N}(t) \approx \mathbf{R}_X(-\epsilon)\mathbf{R}\left(\begin{pmatrix} \Delta\epsilon \\ 0 \\ \Delta\psi \end{pmatrix}\right)\mathbf{R}_X(\epsilon)\mathbf{R}_Z(-\alpha_E)$$

The nutations $\Delta\psi$ and $\Delta\epsilon$ are applied in ecliptic coordinates, with $\mathbf{R}_X(\epsilon)$ representing a transformation into ecliptic coordinates, and $\mathbf{R}_X(-\epsilon)$ representing a transformation back to equatorial coordinates. By using Eq. (4) with $\mathbf{R}_X(-\epsilon)$ as \mathbf{M} , the nutation matrix may be reduced to a series of small rotations:

$$\mathbf{N}(t) \approx \mathbf{R}\left(\begin{pmatrix} \Delta\epsilon \\ -\Delta\psi \sin \epsilon \\ \Delta\psi \cos \epsilon \end{pmatrix}\right)\mathbf{R}_Z(-\alpha_E)$$

By using the explicit form [Eq. (10)] for the equation of the equinoxes, and by collecting together small rotations by using Eq. (5), the approximation

$$\mathbf{N}(t) \approx \mathbf{R}\left(\begin{pmatrix} \Delta\epsilon \\ -\Delta\psi \sin \epsilon \\ 0 \end{pmatrix}\right) \quad (11)$$

is obtained, which is accurate to a few nrad.

When nutation is estimated, the corrected nutation matrix can be represented as

$$\mathbf{N}(t) = \mathbf{N}_{IAU}(t)\mathbf{R}\left(\begin{pmatrix} \delta\epsilon \\ -\delta\psi \sin \epsilon \\ 0 \end{pmatrix}\right) \quad (12)$$

where \mathbf{N}_{IAU} is the (unapproximated) standard model and $\delta\epsilon$ and $\delta\psi$ are corrections to $\Delta\epsilon$ and $\Delta\psi$.

E. Precession

Precession describes the long-term drift of the mean pole of date and mean equinox of date. The mean pole drifts in declination by $n \approx 97.16 \mu\text{rad}$ per Julian year, and the mean equinox drifts in right ascension by $m \approx 223.60 \mu\text{rad}$ per Julian year [13]. The standard model for the precession is given in the form

$$\mathbf{P}(t) = \mathbf{R}_Z(\zeta_A)\mathbf{R}_Y(-\theta_A)\mathbf{R}_Z(z_A) \quad (13)$$

Polynomial expressions for the angles ζ_A , θ_A , and z_A as a function of t are given by Lieske [13,14]. These are, however, physically uninformative. A clearer vectorial formulation of precession is given by Fabri [15].

When corrections to the standard precession model are estimated, the corrected precession matrix may be represented as [16]

$$\mathbf{P}(t) = \mathbf{P}_{IAU}(t)\mathbf{R}\left(\begin{pmatrix} 0 \\ -\delta n \\ \delta m \end{pmatrix}(t - t_D)\right) \quad (14)$$

where \mathbf{P}_{IAU} is the standard model [Eq. (13) with Lieske's polynomials]; δn and δm are corrections to the precession rates in declination and right ascension, respectively; and t_D is a reference epoch, which is preferably near the mean data epoch. The corrections to the general precession in

declination and right ascension, δn and δm , may be expressed as

$$\begin{aligned}\delta n &= \delta p_1 \sin \epsilon \\ \delta m &= \delta p_1 \cos \epsilon - \delta \dot{\chi}\end{aligned}\quad (15)$$

with ϵ representing the mean obliquity of the ecliptic, δp_1 representing the correction to the luni-solar precession in

longitude, and $\delta \dot{\chi}$ representing the correction to the planetary precession in right ascension.

F. The Total Effect of Estimated Quantities

By combining the above results and using Eqs. (4) and (5), one finds that the transformation from terrestrial to celestial coordinates, including estimated quantities, may be expressed as

$$\mathbf{PNSO} = \mathbf{P}_{IAU} \mathbf{N}_{IAU} \mathbf{S}_0 \mathbf{R}(\tilde{\Theta}) \quad (16)$$

where

$$\tilde{\Theta} = \mathbf{S}_0^{-1} \mathbf{N}_{IAU}^{-1} \begin{pmatrix} 0 \\ -\delta n \\ \delta m \end{pmatrix} (t - t_D) + \mathbf{S}_0^{-1} \begin{pmatrix} \delta \epsilon \\ -\delta \psi \sin \epsilon \\ 0 \end{pmatrix} + \begin{pmatrix} y \\ x \\ \Omega(\text{UTC} - \text{UT1}) \end{pmatrix} \quad (17)$$

or, neglecting the effect of the nutation matrix on the precession corrections (this is less than 0.1 nrad),

$$\tilde{\Theta} = \begin{pmatrix} \delta \epsilon \cos \theta_G - (\delta n(t - t_D) + \delta \psi \sin \epsilon) \sin \theta_G + y \\ -\delta \epsilon \sin \theta_G - (\delta n(t - t_D) + \delta \psi \sin \epsilon) \cos \theta_G + x \\ \delta m(t - t_D) + \Omega(\text{UTC} - \text{UT1}) \end{pmatrix} \quad (18)$$

Several points should be noted from this relationship. First, estimation of precession in declination δn is equivalent to estimating a linear trend in the nutation in longitude $\delta \psi$. It can therefore be neglected in the following analysis without loss of generality. Second, estimation of precession in right ascension δm is equivalent to estimating a trend in UT1-UTC. As has been discussed by Williams and Melbourne [17], when corrections to precession are adopted in the future, the definition of UT1 should be altered so that the UT1 series is continuous. Guinot has gone further by suggesting that rather than referring UT1 to the meridian of the mean equinox, it should be referred to a “nonrotating origin,” which is defined on the instantaneous Earth equator so as to be largely independent of precession and nutation models [18]. In the light of this thinking it makes no sense to estimate the precession in right ascension δm . Finally, it should be noted that on time scales short compared to a day, it is impossible to

distinguish between nutation and polar motion; only three angles are needed to describe a general rotation. In fact, if nutations were allowed to have rapid variations with nearly daily periods, there would be no need for the polar angles x and y . Thus, whatever the conceptual definition of the CEP, its actual implementation results from fitting data to slowly varying nutation and polar motion models.

III. Relating the VLBI, LLR, and Planetary Ephemeris Reference Systems

In this section, the relationships between the celestial and terrestrial reference frames for VLBI and LLR will be discussed. The end result will be an expression relating the radio-planetary frame tie to quantities available from the LLR and VLBI data reductions and the tie between LLR and VLBI terrestrial coordinate systems. The

radio-planetary frame tie will be represented by a rotation vector \vec{A} that relates VLBI celestial coordinates \vec{C}_{VLBI} and planetary ephemeris coordinates \vec{C}_{PE} by

$$\vec{C}_{VLBI} = \mathbf{R}(\vec{A})\vec{C}_{PE} \quad (19)$$

The derivation of the frame tie starts with the planetary ephemeris, as represented by the ephemeris of the Earth (which is the celestial reference frame for LLR), and proceeds in steps to the LLR terrestrial coordinate system, the VLBI terrestrial system, and finally to the VLBI celestial system.

For the LLR data reduction, terrestrial coordinates \vec{X}_{LLR} and celestial coordinates \vec{C}_{PE} are related by

$$\vec{C}_{PE} = \mathbf{P}_{IAU}\mathbf{N}_{IAU}\mathbf{S}_0\mathbf{R}(\vec{\Theta}_{LLR})\vec{X}_{LLR} \quad (20)$$

where $\vec{\Theta}_{LLR}$ has the form of Eq. (18). It should be noted here that many LLR data reductions estimate corrections to the planetary ephemeris. This derivation is limited to the case where no such corrections are estimated and overall orientation variations are absorbed by estimated precession and nutation parameters.

The complete transformation from LLR to VLBI terrestrial coordinates must account for a rotation, translation, and a possible difference of scale. This will be discussed in Section VI. Here the main concern is with the relative orientation of the two coordinate systems. Therefore, in this section the relationship between direction coordinates in the two systems will be represented as

$$\vec{X}_{VLBI} = \mathbf{R}(\vec{R})\vec{X}_{LLR} \quad (21)$$

where the vector \vec{R} parameterizes the rotation between the LLR and VLBI terrestrial coordinate systems.

In the VLBI data analysis, terrestrial coordinates \vec{X}_{VLBI} and celestial coordinates \vec{C}_{VLBI} are related by

$$\vec{C}_{VLBI} = \mathbf{P}_{IAU}\mathbf{N}_{IAU}\mathbf{S}_0\mathbf{R}(\vec{\Theta}_{VLBI})\vec{X}_{VLBI} \quad (22)$$

where $\vec{\Theta}_{VLBI}$ has the form of Eq. (18). The parameterization of $\vec{\Theta}_{VLBI}$ estimated in the VLBI data reduction will be discussed in Section V.

By tracing the coordinate transformation

$$\vec{C}_{VLBI} \leftarrow \vec{X}_{VLBI} \leftarrow \vec{X}_{LLR} \leftarrow \vec{C}_{PE}$$

the planetary-radio frame tie is found to be given by

$$\begin{aligned} \mathbf{R}(\vec{A}) &= \mathbf{P}_{IAU}\mathbf{N}_{IAU}\mathbf{S}_0\mathbf{R}(\vec{\Theta}_{VLBI})\mathbf{R}(\vec{R}) \\ &\times \mathbf{R}(-\vec{\Theta}_{LLR})\mathbf{S}_0^{-1}\mathbf{N}_{IAU}^{-1}\mathbf{P}_{IAU}^{-1} \end{aligned} \quad (23)$$

By using Eq. (4) and Eq. (5), this reduces to

$$\vec{A} = \mathbf{P}_{IAU}\mathbf{N}_{IAU}\mathbf{S}_0[\vec{\Theta}_{VLBI} + \vec{R} - \vec{\Theta}_{LLR}] \quad (24)$$

By neglecting the effect of precession and nutation on small quantities (this is less than 0.5 nrad), the components of this equation are given by

$$\begin{aligned} \begin{pmatrix} A_1 \\ A_2 \end{pmatrix} &= \begin{pmatrix} \delta\epsilon_{VLBI} - \delta\epsilon_{LLR} \\ -(\delta\psi_{VLBI} - \delta\psi_{LLR})\sin\epsilon \end{pmatrix} + \begin{pmatrix} \cos\theta_G & -\sin\theta_G \\ \sin\theta_G & \cos\theta_G \end{pmatrix} \begin{pmatrix} R_1 + y_{VLBI} - y_{LLR} \\ R_2 + x_{VLBI} - x_{LLR} \end{pmatrix} \\ A_3 &= R_3 - \Omega(\text{UT1}_{VLBI} - \text{UT1}_{LLR}) \end{aligned} \quad (25)$$

where precession in declination is included as a trend in $\delta\psi$. As argued earlier, nutation and precession can be separated from polar motion only by requiring that each

be slowly varying. Therefore, the terms in Eq. (25) that are modulated by sinusoids in θ_G , the Greenwich Mean Sidereal Time, must be separately zero. This gives the

bias between the two polar motion series in terms of the terrestrial transformation parameters R_1 and R_2 , which correspond to a displacement of the coordinate pole:

$$\begin{aligned} y_{LLR} - y_{VLBI} &= R_1 \\ x_{LLR} - x_{VLBI} &= R_2 \end{aligned} \quad (26)$$

The frame-tie rotation vector is then given by

$$\vec{A} = \begin{pmatrix} \delta\epsilon_{VLBI} - \delta\epsilon_{LLR} \\ -(\delta\psi_{VLBI} - \delta\psi_{LLR}) \sin \epsilon \\ R_3 - \Omega(UT1_{VLBI} - UT1_{LLR}) \end{pmatrix} \quad (27)$$

Equation (27) shows how a full three-dimensional radio-planetary frame tie may be deduced. Its use requires a comparison of LLR and VLBI nutation and UT1 estimates, and a determination of the transformation between VLBI and LLR terrestrial coordinate systems.

IV. The LLR Solution Set

The LLR solution employed here was provided by Newhall, Williams, and Dickey, and is similar to results published by IERS as solution JPL 90 M 01 [19]. However, for this particular solution, no corrections to the planetary ephemeris were estimated. The solution included twenty years of data from August 1969 to January 1989. Station locations, reflector locations, lunar gravity, lunar ephemeris, nutation, precession, and UT0 parameters were estimated from the LLR data. The planetary ephemeris used in the fit was DE200 [20,21] with an updated lunar ephemeris.

Coefficients were estimated for in-phase corrections for the 9-year and annual nutation terms and both in-phase and out-of-phase 18-year nutation terms. The sum total nutation corrections, including the linear trend to account for precession, may be written as

$$\begin{aligned} \delta\epsilon_{LLR} &= 8.73 \cos l' - 0.97 \cos(2\Omega_n) \\ &\quad + 15.13 \cos \Omega_n + 6.88 \sin \Omega_n \text{ nrad} \\ \delta\psi_{LLR} \sin \epsilon &= -156.98 - 5.14 T \\ &\quad + 8.73 \sin l' - 2.18 \sin(2\Omega_n) \\ &\quad - 16.68 \sin \Omega_n + 5.09 \cos \Omega_n \text{ nrad} \end{aligned} \quad (28)$$

where l' is the mean anomaly of the sun, Ω_n is the mean longitude of the ascending lunar node, and T is the time measured from the epoch J2000 in years.

Plate motion was applied to the stations by using the AM0-2 model of Minster and Jordan [22]. This model is based on geological data, and consists of rotation rates for the crustal plates. The model imposes a global condition of “no net rotation” to define absolute site velocities. In the data reduction, the station locations for the epoch 1988.0 were estimated. The resulting estimates are given in Table 1.

V. The VLBI Solution Set

The JPL VLBI software [23] was used to analyze a selected set of NASA’s Deep Space Network (DSN) Catalog Maintenance and Enhancement (CM&E) data and Time and Earth Motion Precision Observations (TEMPO) data. CM&E passes are long observation sessions (12–24 hr) used for the determination of radio source positions, while TEMPO passes are shorter sessions (2–4 hr) used to update Earth orientation. With only three station complexes in the DSN (California, Spain, and Australia), measurements are generally only made on one intercontinental baseline at a time. Two problems occur when measurements are made on one baseline only. First, the component of the total rotation $\vec{\Theta}_{VLBI}$ of Eq. (18) that is along the baseline direction is unobservable. The second problem has to do with determining the angle between the Spain–California and California–Australia baselines. If the observations on these baselines are independent, then this angle cannot be determined. By adding a constant bias to x , y , or UT1 for the sessions on the Spain–California baseline, but not to those for the California–Australia baseline, this angle may be arbitrarily changed.

The strategy adopted here to solve these two problems was to work entirely with pairs of back-to-back Spain–California and California–Australia baseline sessions and to constrain the changes in nutation, UT1, and polar motion between the sessions of any pair to physically reasonable levels. All catalog session pairs with fewer than 24 hours of separation were included. TEMPO session pairs with fewer than 24 hours of separation were included only if they coincided with LLR measurements. From these data, a set of epoch 1988 DSN station locations and a series of nutation corrections, UT1 corrections, and polar motion corrections were estimated. Radio source positions were taken from the JPL radio source catalog 1989-5, which agrees to 5 nrad with IERS celestial reference frame

RSC 89 C 01 [6]. No adjustments were made to the source positions.

For each catalog development session, nutation corrections $\delta\psi$ and $\delta\epsilon$, UT1 corrections δUT1 , and polar motion corrections δx and δy were estimated. The nutation corrections were relative to the standard IAU 1980 series, while the UT1 and polar motion corrections were relative to an a priori series. Changes in these corrections between sessions in a back-to-back pair were constrained (in a least squares sense) to 5 nrad in nutation, 5 nrad in polar motion and 0.2 ms in UT1, which corresponds to the level of random fluctuations of these parameters over one day [24]. The TEMPO sessions are too short to separate nutation from polar motion. An initial solution that did not include TEMPO sessions showed that the nutation corrections for the catalog sessions were 25 nrad or less. In the final solution, therefore, the nutation offsets for the TEMPO sessions were constrained to be zero with 25-nrad sigmas. In all other aspects the TEMPO sessions were modeled identically to the catalog development sessions.

Epoch 1988.0 locations were estimated for all the DSN stations involved in the observations, with constraints from short baseline experiments applied to intracomplex vectors. The motion of the stations was described by the AM0-2 plate motion model. A priori epoch station locations for DSS 14, DSS 43, and DSS 63 were taken from the IERS station set ITRF88 [6]. In order to specify the coordinate system for the adjusted station location set, a rotation and a translation vector between the a priori and adjusted station coordinates were defined. The rotation vector \vec{R} , the translation vector \vec{T} , and a scale change D were defined in terms of an unweighted least-squares fit between the a priori station locations \vec{X}^i and the (as yet uncalculated) adjusted station locations $\vec{X}^i + \delta\vec{X}^i$. This fit results from minimizing

$$J = \sum_{i=14,43,63} \left| \vec{T} - \vec{R} \times \vec{X}^i + D\vec{X}^i - \delta\vec{X}^i \right|^2 \quad (29)$$

Minimization of J with respect to \vec{T} , \vec{R} , and D resulted in a set of linear equations that gives these fit parameters in terms of the station coordinate adjustments $\delta\vec{X}^i$. The translation \vec{T} , and rotation \vec{R} , defined in this manner, were constrained to be zero. The scale change D was left unconstrained. The estimated scale change value was $-9 \pm 4 \times 10^{-9}$.

The station location set resulting from this estimation is given in Table 2. The nutation, UT1, and polar motion estimates are presented in Table 3.

VI. Determination of the DSN VLBI–LLR Station Coordinate Transformation

Since the DSN stations and LLR sites are widely separated, it is necessary to use other data sets to compare the two coordinate systems. The CDP has been performing a number of collocations of SLR and VLBI instruments in order to be able to compare and unify terrestrial reference frames. The results of their comparison indicate agreement between the CDP VLBI terrestrial system and the SLR terrestrial system at the 2-cm level for relative station locations [5]. SLR data are sensitive to the locations of stations with respect to the Earth's center of mass, while VLBI data are insensitive to the geocenter. The collocations of VLBI and SLR instruments allow the SLR geocenter determination to be applied to the VLBI terrestrial frame. Three of the SLR sites used in the VLBI–SLR collocation study are also the LLR sites listed in Table 1. The CDP VLBI solution, therefore, includes the LLR sites as well as the DSN sites. Thus, one can find the relative orientation of the LLR and DSN VLBI terrestrial frames by comparing them with the CDP VLBI solution.

In fitting the station sets it was assumed that each station set (LLR, DSN VLBI, and CDP VLBI) is internally consistent but expressed in a different coordinate system. By using the least-squares procedure described below, a seven-parameter transformation was estimated to map the LLR, DSN VLBI, and CDP VLBI terrestrial systems to a unified terrestrial frame constrained to agree with the CDP VLBI frame in orientation, scale, and translation. The transformation estimates were based on the station coordinates in the station location sets and on ground tie information.

Since there are only three LLR and three DSN VLBI sites used to estimate a seven-parameter transformation, there is more susceptibility to systematic errors than desirable. However, given the good agreement of the SLR and CDP VLBI station sets at the centimeter level and the good agreement in modeling for station locations in the CDP VLBI, SLR, LLR, and DSN VLBI software, the authors do not expect any significant systematic error at the 5- to 10-cm level, which is the accuracy of the LLR station location determination. As more LLR sites become active (recently Wettzell started taking LLR data), it will be possible to strengthen the terrestrial comparison.

The transformations between the station coordinate systems and the unifying coordinate system were assumed to be linear. The transformations included possible offsets of origins and possible rotations. In addition they included possible differences in scale. Scale differences can arise due

to differing treatments of general relativistic corrections. In particular, both the CDP VLBI and DSN VLBI station sets were adjusted to the geocentric metric preferred by IERS [25], while the LLR station locations are expressed with respect to a heliocentric metric [26]. Thus, the LLR terrestrial frame is expected to be different in scale by about 1.5×10^{-8} .

In the fit, the coordinate vector of the i th station in the j th station set (either LLR, DSN VLBI, or CDP VLBI) \vec{X}_j^i is given in terms of \vec{X}_{UCS}^i , the coordinate vector in the unified coordinate system, by

$$\vec{X}_j^i = \vec{T}_j + (1 + D_j)\vec{X}_{UCS}^i - \vec{R}_j \times \vec{X}_{UCS}^i + \vec{W}_j^i \quad (30)$$

where \vec{T}_j is the origin offset of coordinate system j , D_j is the scale offset of coordinate system j , and \vec{R}_j is the rotation offset vector of the j th station set coordinate system. \vec{W}_j^i is the measurement noise on the coordinate vector, which was assumed to be independent for each Cartesian component. The unified coordinate system was defined by constraining \vec{T}_{CDP} , D_{CDP} , and \vec{R}_{CDP} to be zero.

Ground ties are measurements of the displacement between nearby sites, where “nearby” means that the distance between sites is short enough that the errors caused by differences in orientation and scale between coordinate systems are smaller than measurement errors. In this analysis, ground ties were incorporated as measurements of differences between the coordinates of stations in the unified coordinate system. A tie \vec{E}^{ik} between station i and station k was modeled as

$$\vec{E}^{ik} = \vec{X}_{UCS}^i - \vec{X}_{UCS}^k + \vec{V}^{ik} \quad (31)$$

where \vec{X}_{UCS}^i and \vec{X}_{UCS}^k are the station coordinates in the unified system, and \vec{V}^{ik} is the measurement noise, which was assumed to be independent for each Cartesian component.

The estimation procedure used the ground ties and the Cartesian coordinates for each station location set to solve for the transformation parameters. Only diagonal errors were used for coordinates and ties since full covariances were not available for each station set and ground tie. The station locations and errors for the LLR solution are given in Table 1. The DSN VLBI solution station locations and errors are given in Table 2. The station location and formal errors for the CDP station locations used are given in Table 4. Table 5 shows the ground ties used and their

assumed errors. A priori values for transformation parameters for the LLR and DSN VLBI frames were taken as zero with a priori errors set to 100 km for the translation, 1.0 for the scale, and 1 radian for the rotation.

The transformation parameters estimated between the CDP VLBI terrestrial system and the LLR and DSN VLBI terrestrial systems are given in Table 6. Note that the rotations for both LLR and DSN VLBI terrestrial systems are smaller than 10-nrad. This indicates that each terrestrial system is in agreement with the IERS system at the 10-nrad level. The origin of the DSN VLBI system, which was set to agree with the IERS terrestrial reference system ITRF88, is consistent with the CDP VLBI origin, constrained to the ITRF89 terrestrial system, at the few-cm level, which is about the level of uncertainty of the DSN VLBI station location determination. Unlike the VLBI measurements, LLR data are sensitive to the geocenter. The LLR translation offset at the 5- to 10-cm level thus shows agreement of the determination of the geocenter for the LLR and IERS systems at about the LLR uncertainty level.

The overall fit had a χ^2 per degree of freedom of approximately 0.7, indicating that station sets are well fit by the seven-parameter transformation. The fit residuals for the station locations and the ground ties are given in Tables 7 and 8.

The rotation transformation parameters in Table 6 give the rotation from the CDP terrestrial system to either the LLR or DSN VLBI system. For the frame tie one needs the rotation from the LLR terrestrial system to the DSN VLBI system, which is given by

$$\vec{R} = \begin{pmatrix} - & 11 \pm 22 \\ + & 4 \pm 16 \\ - & 3 \pm 7 \end{pmatrix} \text{ nrad} \quad (32)$$

VII. The Planetary-Radio Frame Tie

Comparisons of the LLR and DSN VLBI nutation corrections and UT1 series are presented in this section. In accordance with the analysis in Section III, the planetary-radio frame tie is then synthesized from the derived biases between the LLR and DSN VLBI nutation and UT1 series, and results that have been presented above.

A. Comparison of LLR and DSN VLBI Nutation Corrections

Equation (27) shows that the x and y components of the frame tie rotation vector \vec{A} , which correspond to an offset between the planetary ephemeris and radio catalog coordinate poles, are related to the bias between the LLR and DSN VLBI nutation corrections. The DSN VLBI and LLR corrections to the IAU nutation theory are compared in Figs. 1 and 2, with Fig. 1 showing corrections to $\Delta\epsilon$ and Fig. 2 showing corrections to $\Delta\psi \sin \epsilon$. The points with error bars are the DSN VLBI estimates. They come in pairs, one for each session in a back-to-back session pair. The points with large errors in the late 1980s are the TEMPO sessions. The solid lines represent the LLR nutation corrections as given by Eq. (28). For ease of comparison, the best-fit VLBI–LLR offset has been added to each of the LLR curves. The biases were found to be

$$\begin{aligned} \delta\epsilon_{VLBI} - \delta\epsilon_{LLR} &= 5 \pm 10 \text{ nrad} \\ (\delta\psi_{VLBI} - \delta\psi_{LLR}) \sin \epsilon &= -49 \pm 10 \text{ nrad} \end{aligned} \quad (33)$$

The fits, which were performed by neglecting the errors in the LLR corrections, resulted in formal bias errors near 1 nrad. Correct treatment of the LLR nutation errors is problematic. Williams, Newhall, and Dickey [27] quote separate uncertainties of 10 nrad for the 18.6-year nutation amplitudes and 1.2 nrad/year for the precession in declination as measured by LLR. However, what matters here is the accuracy of the total nutation correction at epochs within the data span. This total should be better determined than any of its component parts. The errors given in Eq. (33) reflect the authors' estimate of the uncertainty of the LLR corrections.

B. Comparison of LLR and DSN VLBI UT1 Series

As was shown in Section III, the planetary-radio frame tie in right ascension consists of two offsets. The first offset is R_3 , the difference in longitude origin of the two terrestrial coordinate systems. The second offset arises from a bias between the VLBI and LLR UT1 series and is considered here.

The DSN VLBI solutions for UT1 and polar motion have already been presented in Table 3. Table 9 presents those LLR measurements that occurred near one of the pairs of VLBI session pairs. In some instances no LLR measurements occurred near a session pair, and in others several measurements occurred. For the LLR reduction,

only UT0 was estimated. Table 9 shows the time and date, estimated UT0–UTC and its error, the polar motion angles x_0 and y_0 assumed in the reduction, the sensitivity S_x and S_y of UT0 to the polar motion angles, and the LLR station name.

A corrected value of UT0 for the LLR measurements, to include updated polar motion values, was modeled as

$$\begin{aligned} \text{UT0}_{LLR}^{corr} &= \text{UT0}_{LLR} + [S_x(x_{LLR} - x_0) \\ &\quad + S_y(y_{LLR} - y_0)]/\Omega \end{aligned} \quad (34)$$

where UT0_{LLR} is the value estimated in the LLR reduction by using polar motion values x_0 and y_0 , UT0_{LLR}^{corr} is the value that would result if the LLR reduction had used updated polar motion values x_{LLR} and y_{LLR} , and Ω is the mean rotation rate of the Earth. The updated LLR polar motion angles were obtained from the DSN VLBI analysis with corrections given by Eq. (26):

$$x_{LLR} = x_{VLBI} + R_2, \quad y_{LLR} = y_{VLBI} + R_1$$

where x_{VLBI} and y_{VLBI} are the polar motion values from the DSN VLBI fit interpolated to the time of the LLR measurement, and R_1 and R_2 are VLBI–LLR terrestrial coordinate rotations about the x - and y -axis presented in Section VI.

UT1 is given in terms of UT0 and polar motion by

$$\begin{aligned} \text{UT1}_{LLR} &= \text{UT0}_{LLR}^{corr} - \tan \phi [x_{LLR} \sin \lambda \\ &\quad + y_{LLR} \cos \lambda]/\Omega \end{aligned} \quad (35)$$

where ϕ and λ are the latitude and longitude of the LLR station.

Using all DSN VLBI session pairs with coincident LLR measurements, a least-squares fit was performed to estimate the bias, ΔUT1 , between DSN VLBI and the LLR UT1, as defined by

$$\text{UT1}_{LLR} = \text{UT1}_{VLBI} - \Delta\text{UT1} \quad (36)$$

where UT1_{VLBI} is the DSN VLBI UT1 determination interpolated to the time of the LLR measurement.

The least-squares fit using the LLR measurements for all back-to-back DSN VLBI session pairs incorporated the full six-by-six information matrix for the two sets of VLBI UT/PM estimates in each back-to-back session pair. The offset ΔUT1 was estimated, and the sensitivity of this estimate to the rotations R_1 and R_2 was calculated. The resulting offset measurements are shown in Fig. 3. The weighted mean offset was found to be

$$\text{UT1}_{\text{VLBI}} - \text{UT1}_{\text{LLR}} = 0.22 \pm 0.12 \text{ msec} \quad (37)$$

where the error given here includes the considered effect of the errors in the rotations R_1 and R_2 .

C. The Frame Tie

By returning to Eq. (27) and substituting the terrestrial rotation, nutation, and UT1 biases given above, the following estimate of the frame tie from the ephemeris DE200 to the IERS celestial reference frame results:

$$\vec{A} = \begin{pmatrix} + 5 \pm 15 \\ - 49 \pm 15 \\ - 19 \pm 25 \end{pmatrix} \text{ nrad} \quad (38)$$

The errors from the comparison process include the nutation bias uncertainties (10 nrad), the UT bias uncertainty (9 nrad), the R_3 uncertainty (7 nrad), and the uncertainty in the alignment of the radio source catalog with the IERS celestial reference frame (5 nrad in each component). The errors given in Eq. (38) include estimates of systematic errors. Since many steps in the comparison procedure rely on separate data reductions, each with correlated parameters, to derive formal errors would require combining full covariance matrices, not all of which are available. The largest potential source of systematic error is thought to lie in the comparison of the UT1 series where the number of points included is small for a measurement known to be fairly noisy. In future work, more comparison points can be obtained by including a more extensive VLBI data set. Other improvements could come from combining the LLR and VLBI information matrices [28], along with the full covariance for the CDP station determination, to allow an estimate of the errors including correlations of parameters. However, the presented frame tie result is apparently the most global and accurate determination yet available.

The frame tie result given in Eq. (38) represents the rotation (and uncertainty) between the IERS radio source

frame and the reference frame determined by the tabulated orbit of the Earth within the ephemeris DE200. The orbit of the Earth is tabulated with respect to a projected dynamical equator and equinox for the year 2000 [20]. There is significant uncertainty in the determination of the equinox of 2000 since it depends upon predictions using estimated precession and nutation constants, which are quantities that (aside from data reduction) do not affect the orbits of the planets. The authors believe that the physical content of the ephemeris can be referred to the orbit of the Earth for the definition of the reference system. The orbits of the other planets do not define different reference systems but can instead be referred to the orbit of the Earth with an uncertainty characteristic of the internal consistency of the ephemeris.

VIII. Comparison With Other Frame Tie Determinations

Other methods of determining the radio-planetary frame tie include VLBI observation of spacecraft at other planets and comparison of positions of millisecond pulsars based on VLBI and timing measurements. The result presented above in Eq. (38) can be compared with other results by examining the offset in right ascension and declination in the part of the sky where the other measurements exist.

There have been a number of VLBI observations of spacecraft at other planets. A planetary orbiter, or a spacecraft making a planetary encounter, has a position determined with respect to the planet from the gravitational signature on the spacecraft Doppler data. VLBI measurements between the spacecraft and one or more angularly nearby radio sources can be used to estimate the radio source coordinates in the planetary reference frame. Newhall, Preston, and Esposito [29] reported average right ascension and declination offsets consistent with zero, with uncertainty of 40–60 nrad, based on the results of VLBI measurements for the Viking and Pioneer Venus orbiters. McElreath and Bhat [30] derived a position of the radio source P 0202 + 14 in the planetary ephemeris frame from observations of the Soviet Vega 1 and Vega 2 spacecraft as they flew by Venus in 1985. The Vega measurements resulted in right ascension and declination offsets consistent with Eq. (38) within their errors of 50 nrad in each component. In 1989, VLBI observations of the Soviet Phobos spacecraft at Mars were made for frame tie determination in nearly the same part of the sky as the Vega observations. Preliminary results of the Phobos data⁴ are consis-

⁴ B. A. Iijima and C. E. Hildebrand, personal communication, Jet Propulsion Laboratory, Pasadena, California, 1991.

tent with the results in Eq. (38) at the 1-sigma level. An observation sequence for the Magellan spacecraft at Venus is being pursued to extend the data set of VLBI spacecraft observations.

Timing of millisecond pulsars gives positions with few-nrad accuracy based on the orbit of the Earth [31]. VLBI observations of these sources are difficult since the pulsars are weak radio sources. Two groups^{5,6} have made VLBI observations of the pulsar PSR 1937+21. Preliminary results from one group⁶ give right ascension and declination offsets in agreement with Eq. (38) within their errors.

In the future more spacecraft VLBI measurements and refinements of the technique presented here, as well as results from other methods, should combine to produce a consistent frame tie determination at the 5-nrad level. In the meantime, the radio-planetary frame tie result presented here with 15–25 nrad accuracy is a useful reference point.

IX. Application to Interplanetary Spacecraft Navigation

In order to apply this (or any other) frame tie result to spacecraft navigation with full accuracy, it will be necessary to have well-defined standards for reference frame definition. Guidelines for standards and implementation are proposed below.

For orbit determination, UT and polar motion are usually read in from an external service and not adjusted (or estimated) in the navigation process. The importance of this external UTPM information in defining the reference frame for the spacecraft is often overlooked. The adoption of a station set and an Earth orientation series essentially defines a celestial reference frame that may be different from the desired reference frame (often the planetary ephemeris reference frame). This inconsistency is most important for interplanetary missions tracked mainly by Doppler. In this case, the signature of the Earth on the Doppler data is tied most strongly to a celestial reference frame that is defined by the station set and Earth orientation series. When there are data directly sensitive to the planetary ephemeris, such as range (which is sensitive to the orbit of the Earth) or onboard optical data, there can be a systematic discrepancy among the various data types

which will be resolved by the amount and weighting of the data.

It is preferable to clearly define the reference frames in use rather than having them defined implicitly and/or inconsistently. The most practical choice would be to use the IERS definitions for station locations, Earth orientation, and quasar locations while allowing the planetary ephemeris to define its own reference system. Each ephemeris would be related to the standard celestial coordinate system by three rotation angles, such as those given in Eq. (38). This choice of standards would simplify matters by minimizing the number of parameters that would vary from mission to mission or from ephemeris to ephemeris. Each mission could use a standard station set, Earth orientation series, and quasar catalog, regardless of the ephemeris used. A priori values for the three rotation angles could be adopted from an external determination (such as reported in this work). If it is desired and the necessary partials exist, corrections to the frame tie could be estimated for a particular orbit determination analysis.

This work has utilized the high accuracy of terrestrial station locations in determining the frame tie. Geocentric station locations have been determined with accuracy better than 10 cm in all components. Each aspect of the station location determination has been checked by independent data sets and reduction software. VLBI and SLR each produce relative station locations with 2- to 3-cm accuracy. SLR and LLR independently determine the geocenter to 10-cm accuracy or better. The time dependence of the DSN station locations (i.e., plate motion) and the rotation of the station locations into inertial space are also well known. There is no reason that interplanetary spacecraft navigation cannot take advantage of these high-accuracy station locations.

X. Conclusion

A determination of the rotational offset between the planetary ephemeris DE200 and the radio reference frame has been presented based on a comparison of VLBI and LLR Earth orientation measurements. The accuracy of the frame tie is about 25 nrad. The frame tie result is substantiated by comparison with determinations from other techniques. The frame tie result is made possible by the ability to determine the location of DSN tracking stations with accuracy better than 10 cm. The frame tie result, combined with proper use of accurate station locations, will enable more accurate interplanetary spacecraft navigation.

⁵ N. Bartel, personal communication, Harvard-Smithsonian Center for Astrophysics, Cambridge, Massachusetts, April 9, 1991.

⁶ R. J. Dewey and D. L. Jones, "Millisecond Pulsar Frame Tie," JPL IOM 335-6-91-006, (internal document) Jet Propulsion Laboratory, Pasadena, California, April 17, 1991.

Acknowledgments

The authors would like to thank Skip Newhall, Allan Steppe, Ojars Sovers, and Jim Williams for many hours of useful discussion. They also would like to acknowledge the careful and very useful review of this work provided by Roger Linfield. Jim Ray graciously provided results on terrestrial frame comparisons at many stages of this work.

References

- [1] J. S. Border, F. F. Donovan, S. G. Finley, C. E. Hildebrand, B. Moultrie, and L. J. Skjerve, "Determining Spacecraft Angular Position with Delta VLBI: The Voyager Demonstration," paper AIAA-82-1471, presented at the AIAA/AAS Astrodynamics Conference, San Diego, California, August 9–11, 1982.
- [2] O. J. Sovers, "JPL 1990-3: A 5-nrad Extragalactic Source Catalog Based on Combined Radio Interferometric Observations," *TDA Progress Report 42-106*, vol. April–June 1991, Jet Propulsion Laboratory, Pasadena, California, pp. 364–383, August 15, 1991.
- [3] J. G. Williams and E. M. Standish, "Dynamical Reference Frames in the Planetary and Earth-Moon Systems," in *Reference Frames in Astronomy and Geophysics*, edited by J. Kovalevsky et al., Boston: Kluwer Academic Publishers, pp. 67–90, 1989.
- [4] C. S. Christensen, S. W. Thurman, J. M. Davidson, M. H. Finger, and W. M. Folkner, "High-Precision Radiometric Tracking for Planetary Approach and Encounter in the Inner Solar System," *TDA Progress Report 42-97*, vol. January–March 1989, Jet Propulsion Laboratory, Pasadena, California, pp. 21–46, May 15, 1990.
- [5] J. R. Ray, C. Ma, T. A. Clark, J. W. Ryan, R. J. Eanes, M. M. Watkins, B. E. Schutz, and B. D. Tapley, "Comparison of VLBI and SLR Geocentric Site Coordinates," *Geophys. Res. Lett.*, vol. 18, pp. 231–234, 1991.
- [6] *International Earth Rotation Service, Annual Report for 1988*, Observatoire de Paris, France, 1989.
- [7] Z. Altamimi, E. F. Arias, C. Boucher, and M. Feissel, "Earth Orientation Determinations: Some Tests of Consistency," paper presented at the 105th Symposium on Earth Rotation and Coordinate Reference Frames, Edinburgh, Scotland, August 10–11, 1989.
- [8] C. Boucher and Z. Altamimi, "The Initial IERS Terrestrial Reference Frame," IERS Technical Note 1, Observatoire de Paris, France, 1989.
- [9] P. K. Seidelmann, "1980 IAU Theory of Nutation: The Final Report of the IAU Working Group on Nutation," *Celestial Mechanics*, vol. 27, pp. 79–106, 1982.
- [10] N. Capitaine, J. G. Williams, and P. K. Seidelmann, "Clarifications Concerning the Definition of the Celestial Ephemeris Pole," *Astron. Astrophys.*, vol. 146, pp. 381–383, 1985.

- [11] S. Aoki, B. Guinot, G. H. Kaplan, H. Kinoshita, D. D. McCarthy, and P. K. Seidelmann, "The New Definition of Universal Time," *Astron. Astrophys.*, vol. 105, pp. 359–361, 1982.
- [12] J. M. Wahr, "The Forced Nutations of an Elliptical, Rotating, Elastic and Oceanless Earth," *Geophys. J. R. Astr. Soc.*, vol. 64, pp. 705–727, 1981.
- [13] J. H. Lieske, T. Lederle, W. Fricke, B. Morando, "Expressions for the Precession Quantities Based upon the IAU (1976) System of Astronomical Constants," *Astron. Astrophys.*, vol. 58, pp. 1–16, 1977.
- [14] J. H. Lieske, "Precession Matrix Based on IAU (1976) System of Astronomical Constants," *Astron. Astrophys.*, vol. 73, pp. 283–284, 1979.
- [15] E. Fabri, "Advocating the Use of Vector-Matrix Notation in Precession Theory," *Astron. Astrophys.*, vol. 82, pp. 123–128, 1980.
- [16] S. Y. Zhu and I. I. Mueller, "Effects of Adopting New Precession, Nutation and Equinox Corrections on the Terrestrial Reference Frame," *Bulletin Geodesique*, vol. 57, pp. 29–42, 1983.
- [17] J. G. Williams and W. G. Melbourne, "Comments on the Effect of Adopting New Precession and Equinox Corrections," in *High-Precision Earth Rotation and Earth-Moon Dynamics*, edited by O. Calame, Boston: D. Reidel, pp. 293–303, 1982.
- [18] N. Capitaine, B. Guinot, and J. Souchay, "A Non-Rotating Origin on the Instantaneous Equator: Definition, Properties, and Use," *Celestial Mechanics*, vol. 39, pp. 283–307, 1986.
- [19] X X Newhall, J. G. Williams, and J. O. Dickey, "Earth Rotation (UT0) From Lunar Laser Ranging," IERS Technical Note 5, Observatoire de Paris, France, pp. 41–44, 1990.
- [20] E. M. Standish, Jr., "Orientation of the JPL Ephemerides, DE200/LE200, to the Dynamical Equinox of J2000," *Astron. Astrophys.*, vol. 114, pp. 297–302, 1982.
- [21] E. M. Standish, Jr., "The Observational Basis for JPL's DE200, the Planetary Ephemeris of the Astronomical Almanac," *Astron. Astrophys.*, vol. 233, pp. 252–271, 1990.
- [22] J. B. Minster and T. H. Jordan, "Present Day Plate Motions," *J. Geophys. Res.*, vol. 83, pp. 5331–5354, 1978.
- [23] O. J. Sovers, *Observation Model and Parameter Partial for the JPL VLBI Parameter Estimation Software MODEST—1991*, JPL Publication 83-39, Rev. 4, Jet Propulsion Laboratory, Pasadena, California, August 1, 1991.
- [24] D. D. Morabito, T. M. Eubanks, and J. A. Steppe, "Kalman Filtering of Earth Orientation Changes," in *Earth's Rotation and Reference Frames for Geodesy and Geodynamics*, edited by A. H. Babcock and G. A. Wilkens, Dordrecht, The Netherlands: D. Reidel, pp. 257–267, 1988.
- [25] D. D. McCarthy, "IERS Standards (1989)," IERS Technical Note 3, Observatoire de Paris, France, 1989.
- [26] R. W. Hellings, "Relativistic Effects in Astronomical Timing Measurements," *Astronomical J.*, vol. 91, pp. 650–659, 1986.
- [27] J. G. Williams, X X Newhall, and J. O. Dickey, "Luni-Solar Precession: Determination from Lunar Laser Ranges," *Astron. Astrophys.*, vol. 241, pp. L9–L12, 1991.

- [28] P. Charlot, O. J. Sovers, J. G. Williams, and X X Newhall, "A Global VLBI/LLR Analysis for the Determination of Precession and Nutation Constants," in *Reference Systems: Proceedings of the 127th Colloquium of the International Astronomical Union*, edited by J. A. Hughes, C. A. Smith, and G. H. Kaplan, Washington, DC: U.S. Naval Observatory, pp. 228–233, 1991.
- [29] X X Newhall, R. A. Preston, and P. B. Esposito, "Relating the JPL VLBI Reference Frame and the Planetary Ephemerides," *Proceedings of the 109th Symposium of the IAU on Astrometric Techniques*, edited by H. K. Eichorn and R. J. Leacock, Boston: Reidel, pp. 789–794, 1986.
- [30] T. P. McElrath and R. S. Bhat, "Determination of the Inner Planet Frame Tie Using VLBI Data," paper 88-4234, presented at the AIAA/AAS Astrodynamics Conference, Minneapolis, Minnesota, 1988.
- [31] L. A. Rawley, J. H. Taylor, and M. M. Davis, "Fundamental Astrometry and Millisecond Pulsars," *Astrophys. J.*, vol. 326, pp. 947–953, 1988.

Table 1. Lunar Laser Ranging station coordinates.

Station	No.	x , m	y , m	z , m	σ_x , m	σ_y , m	σ_z , m
McDonald 107-in.	7206	-1330781.1660	-5328755.6310	3235697.6320	0.0300	0.0300	0.1000
McDonald MLRS ^a	0108	-1330120.9160	-5328532.2060	3236146.6410	0.0300	0.0300	0.1000
Haleakala	0210	-5466006.9080	-2404428.1360	2242188.5400	0.0300	0.0300	0.1000
Grasse	7845	4581692.2540	556195.8208	4389354.8430	0.0300	0.0300	0.1000

^a MLRS = McDonald Laser Ranging System.

Table 2. DSN VLBI station coordinates.

Station	No.	x , m	y , m	z , m	σ_x , m	σ_y , m	σ_z , m
DSS 14	1514	-2353621.0830	-4641341.5930	3677052.3000	0.0312	0.0318	0.0315
DSS 43	1543	-4460894.4630	2682361.6260	-3674748.7600	0.0341	0.0311	0.0317
DSS 63	1563	4849092.7130	-360180.6860	4115108.9730	0.0324	0.0320	0.0338

Table 3. VLBI nutation, polar motion, and UT1 estimates.

Mean date	Time	$\Delta\epsilon$, mas	$\sigma(\Delta\epsilon)$, mas	$\Delta\psi$, mas	$\sigma(\Delta\psi)$, mas	UT1– UTC, ms	$\sigma(\text{UT1–UTC})$ ms	x mas	$\sigma(x)$, mas	y , mas	$\sigma(y)$, mas
Dec. 20, 1979	13:39:24	0.64	0.48	2.40	1.56	–324.83	0.16	150.16	2.23	273.76	0.77
Dec. 21, 1979	16:56:57	0.50	1.05	1.55	2.85	–327.65	0.17	150.18	2.22	271.91	1.20
Jan. 25, 1980	23:37:29	0.87	2.32	2.46	3.44	583.53	0.15	123.28	2.55	214.17	2.69
Jan. 27, 1980	14:44:25	1.01	2.47	1.52	3.42	579.54	0.18	120.90	2.56	211.90	2.52
Feb. 14, 1980	05:02:33	–1.36	0.96	1.86	2.57	539.85	0.09	83.77	1.61	189.25	1.50
Feb. 14, 1980	22:04:27	–1.34	1.16	1.59	2.71	538.03	0.15	82.80	1.71	188.50	1.23
Feb. 23, 1980	18:32:42	0.52	0.56	4.32	1.94	514.35	0.15	73.39	2.16	184.22	0.78
Feb. 24, 1980	12:47:20	0.95	1.09	5.24	3.09	512.45	0.12	72.80	2.14	183.70	1.20
Dec. 8, 1981	16:03:38	2.91	1.26	10.70	5.28	69.45	0.15	–110.76	2.15	324.21	2.01
Dec. 9, 1981	09:45:29	2.51	1.03	10.33	5.01	67.72	0.17	–110.51	2.18	325.74	1.80
May 20, 1983	20:10:50	0.03	0.24	–0.29	0.55	–164.44	0.10	143.35	1.19	542.34	0.42
May 22, 1983	09:05:59	0.08	0.54	–3.42	1.54	–168.12	0.06	150.14	1.00	539.78	0.96
Nov. 18, 1983	10:55:03	2.79	0.49	–7.94	1.71	489.12	0.14	19.05	1.28	19.99	0.81
Nov. 19, 1983	10:09:52	2.56	0.51	–6.53	1.49	486.73	0.09	14.88	1.09	20.67	1.18
Dec. 17, 1983	11:12:20	4.67	0.63	–1.79	1.38	427.56	0.09	–89.02	1.10	59.67	1.15
Dec. 18, 1983	10:00:46	5.33	0.55	–5.61	1.39	425.85	0.13	–92.03	1.27	61.98	0.76
Mar. 24, 1984	22:55:12	0.50	0.56	–0.86	1.29	255.08	0.08	–225.02	1.04	389.58	1.07
Mar. 25, 1984	22:01:27	0.82	0.25	–1.16	0.64	253.06	0.11	–223.82	1.21	393.11	0.63
May 12, 1984	12:02:11	–1.19	0.74	0.02	1.72	161.00	0.10	–84.21	1.34	540.76	1.60
May 13, 1984	04:09:50	–1.00	1.13	–0.49	2.88	159.83	0.18	–81.94	1.52	541.95	1.37
Jul. 14, 1984	14:44:35	0.48	0.83	–7.05	1.55	90.22	0.10	175.04	1.19	520.60	1.24
Jul. 15, 1984	14:23:34	0.70	0.91	–8.32	1.58	89.50	0.13	179.03	1.34	518.19	0.89
Sep. 28, 1985	18:08:45	–0.04	0.78	–14.46	2.03	472.50	0.09	213.43	1.30	411.71	1.06
Sep. 29, 1985	20:52:30	0.61	0.55	–13.42	1.30	470.64	0.13	214.63	1.43	408.48	0.60
Mar. 22, 1986	23:46:10	4.09	3.35	–8.31	8.91	200.13	0.18	–16.50	4.73	125.40	3.62
Mar. 23, 1986	07:44:37	4.23	3.36	–8.77	9.00	199.71	0.22	–17.15	4.70	125.81	3.52
Apr. 19, 1986	12:47:01	1.86	3.74	–2.03	9.58	155.94	0.23	–69.80	4.69	173.06	4.26
Apr. 20, 1986	12:31:53	2.01	3.86	–1.91	9.78	154.45	0.21	–71.56	4.69	174.99	4.36
Jun. 28, 1986	19:00:33	1.53	1.04	–4.07	2.74	75.10	0.12	–70.61	1.96	319.24	1.16
Jun. 29, 1986	20:51:35	1.69	0.52	–4.15	1.49	74.39	0.14	–69.09	1.97	321.68	0.72
Apr. 18, 1987	22:17:11	3.61	3.45	–8.79	10.87	–305.34	0.25	74.90	3.73	206.40	5.54
Apr. 19, 1987	15:30:21	3.52	3.50	–9.08	11.15	–306.40	0.27	73.98	3.77	206.10	5.46
May 9, 1987	09:49:51	–0.61	0.64	–2.26	1.31	–336.87	0.12	54.37	1.26	203.11	0.82
May 10, 1987	19:22:27	–0.77	0.52	–2.81	1.22	–338.75	0.07	52.68	1.06	202.90	1.18
Jan. 9, 1988	10:59:49	3.36	1.62	–8.73	6.99	353.65	0.20	–5.78	3.61	423.26	2.19
Jan. 10, 1988	02:56:59	3.48	1.71	–9.15	7.12	352.66	0.12	–4.69	3.65	423.58	2.31
Oct. 1, 1988	18:10:17	–0.03	2.81	–16.21	7.11	24.15	0.11	9.17	4.63	131.47	2.45
Oct. 1, 1988	22:20:34	0.04	2.93	–15.88	7.14	24.03	0.18	8.41	4.60	131.58	2.33

Table 4. CDP VLBI station coordinates.

Station	No.	x , m	y , m	z , m	σ_x , m	σ_y , m	σ_z , m
DSS 13	1513	-2351128.9948	-4655477.0834	3660956.8432	0.0027	0.0053	0.0047
DSS 45	1645	-4460935.0547	2682765.7891	-3674381.6368	0.0195	0.0130	0.0117
Haleakala	7120	-5465998.3924	-2404408.5665	2242228.4099	0.0142	0.0074	0.0071
DSS 65	1665	4849336.7823	-360488.9205	4114748.5369	0.0125	0.0049	0.0132
Grasse	7605	4581697.8187	556125.6265	4389351.2470	0.0067	0.0026	0.0075
DSS 15	1615	-2353538.6234	-4641649.5275	3676669.9431	0.0044	0.0088	0.0075
McDonald	7850	-1330008.0136	-5328391.5430	3236502.6372	0.0028	0.0102	0.0063

Table 5. Ground tie vectors.

Site	From	To	x , m	y , m	z , m	σ_x , m	σ_y , m	σ_z , m
McDonald ^a	7206	7086	655.9005	229.0262	452.6222	0.0100	0.0100	0.0100
McDonald ^b	7086	0108	4.3560	-5.6310	-3.5570	0.0100	0.0100	0.0100
McDonald ^a	7086	7850	117.2017	135.0619	352.4838	0.0100	0.0100	0.0100
Haleakala ^c	7210	0210	-0.4830	-0.2120	1.0030	0.0100	0.0100	0.0100
Haleakala ^a	7120	7210	-8.0140	-19.4100	-40.9270	0.0100	0.0100	0.0100
Grasse ^a	7835	7845	0.5780	36.4730	-4.4390	0.0100	0.0100	0.0100
Grasse ^d	7605	7835	-6.0150	33.7350	8.1020	0.0100	0.0100	0.0100
Goldstone ^e	1513	1514	-2492.0800	14135.5350	16095.4150	0.0100	0.0100	0.0100
Goldstone ^e	1513	1615	-2409.6220	13827.5670	15713.0940	0.0200	0.0200	0.0210
Madrid ^e	1665	1563	-244.1140	308.2930	360.3200	0.0200	0.0200	0.0200
Canberra ^e	1645	1543	40.6580	-404.1520	-367.1850	0.0100	0.0100	0.0100

^aCrustal Dynamics Project Site Catalog, Goddard Space Flight Center, Greenbelt, Maryland, May, 1989.

^bT. M. Sager and J. L. Long, internal memorandum, Bendix Aerospace Corporation, Columbia, Maryland, April 11, 1985.

^cL. S. Baker, internal memorandum, National Geodetic Survey, Rockville, Maryland, October 24, 1975.

^dC. Boucher, personal communication, Institut Geophysique, St. Mandé, France, April 1990.

^eC. S. Jacobs, personal communication, Jet Propulsion Laboratory, Pasadena, California, December 1989.

Table 6. Transformation parameters from CDP VLBI coordinate system to DSN or LLR system.

System	T_1, cm	T_2, cm	T_3, cm	$D(10^{-9})$	$R_1, \text{ nrad}$	$R_2, \text{ nrad}$	$R_3, \text{ nrad}$
DSN	-0.7 ± 2.3	-2.4 ± 2.3	6.6 ± 2.3	5.5 ± 3.5	-5.2 ± 4.9	-0.5 ± 4.6	-1.5 ± 5.0
LLR	-8.0 ± 6.2	-3.2 ± 7.7	4.3 ± 8.0	-9.8 ± 4.4	6.0 ± 21.5	-4.1 ± 15.0	1.8 ± 5.3

Table 7. Input coordinate residuals.

Site	System	No.	$x, \text{ mm}$	$y, \text{ mm}$	$z, \text{ mm}$
Goldstone	DSN	1514	3.2	25.1	-18.9
Canberra	DSN	1543	-20.2	-11.6	0.4
Madrid	DSN	1563	14.7	-13.1	21.3
McDonald	LLR	7206	10.3	-30.5	51.1
McDonald	LLR	0108	4.5	-3.7	-4.5
Haleakala	LLR	0210	2.2	29.5	-3.2
Grasse	LLR	7845	-17.1	4.7	-43.4
DSS 13	CDP	1513	0.1	0.0	0.2
DSS 45	CDP	1645	6.6	2.0	-0.1
Haleakala	CDP	7120	-0.5	-1.8	0.0
DSS 65	CDP	1665	-2.2	0.3	-3.3
Grasse	CDP	7605	0.8	0.0	0.2
DSS 15	CDP	1615	-0.3	-1.8	0.7
McDonald	CDP	7850	-0.1	4.0	-0.2

Table 8. Ground tie residuals.

Site	From	To	$x, \text{ mm}$	$y, \text{ mm}$	$z, \text{ mm}$
McDonald	7206	7086	1.1	-3.4	0.5
McDonald	7086	0108	-0.5	0.4	0.0
McDonald	7086	7850	1.6	-3.8	0.5
Haleakala	7210	0210	-0.2	-3.3	0.0
Haleakala	7120	7210	-0.2	-3.3	0.0
Grasse	7835	7845	1.9	-0.5	0.4
Grasse	7605	7835	1.9	-0.5	0.4
Goldstone	1513	1514	-0.3	-2.5	1.9
Goldstone	1513	1615	6.2	9.3	-5.3
Madrid	1665	1663	-5.6	5.1	-7.5
Canberra	1645	1543	1.7	1.2	0.0

Table 9. Lunar Laser Ranging estimated UT0.

Date	Time	UT0– UTC ms	UT0– UTC σ , ms	x , mas	y , mas	S_x , mas/mas	S_y , mas/mas	Site
Jan. 26, 1980	03:16:19	573.695	0.304	114.042	213.383	−0.03837	0.15363	McDonald
Jan. 27, 1980	01:00:23	571.010	0.589	112.599	212.143	0.04666	−0.18683	McDonald
Jan. 28, 1980	04:02:20	569.085	0.449	110.804	210.599	0.00398	−0.01595	McDonald
Feb. 24, 1980	02:54:08	506.952	0.469	67.877	181.884	−0.03957	0.15844	McDonald
Feb. 25, 1980	02:28:28	503.540	0.350	66.969	181.103	0.00981	−0.03928	McDonald
Dec. 8, 1981	05:42:44	71.082	0.424	−115.685	324.240	−0.07837	0.31382	McDonald
Dec. 9, 1981	06:09:18	66.559	0.457	−115.550	326.493	−0.05714	0.22880	McDonald
Dec. 10, 1981	04:41:58	65.207	0.266	−115.426	328.571	−0.00842	0.03371	McDonald
Nov. 17, 1983	04:12:40	489.83	0.367	20.977	16.719	0.00295	−0.01182	McDonald
Dec. 17, 1983	05:01:36	430.525	0.598	−92.780	57.207	−0.00951	0.03808	McDonald
May 11, 1984	23:23:32	193.926	0.355	−88.808	536.713	0.62278	−0.07560	Grasse
Jul. 16, 1984	08:37:45	78.004	0.698	178.951	513.587	0.01670	−0.06688	McDonald
Mar. 22, 1986	02:13:30	200.782	0.221	−19.178	124.652	0.07114	−0.28499	MLRS ^a
Mar. 23, 1986	03:01:29	199.584	0.117	−21.201	125.789	0.04375	−0.17528	MLRS
Apr. 18, 1986	20:10:57	167.546	0.151	−71.066	170.577	0.27160	−0.03297	Grasse
Apr. 19, 1986	03:47:27	157.666	0.132	−71.532	171.207	−0.03970	0.15902	MLRS
Apr. 19, 1986	20:58:15	165.807	0.230	−72.629	172.553	0.26490	−0.03216	Grasse
Jun. 29, 1986	14:19:11	65.176	0.253	−74.057	319.475	0.26536	−0.11673	Haleakala
Apr. 19, 1987	14:36:20	313.090	0.385	74.779	204.107	0.10398	−0.04574	Haleakala
Apr. 20, 1987	15:02:45	313.976	0.283	73.923	203.901	0.14778	−0.06501	Haleakala
May 8, 1987	03:57:04	339.732	0.148	55.129	200.679	−0.04213	0.16879	MLRS
May 8, 1987	08:39:43	341.488	0.094	54.920	200.634	−0.13585	0.05976	Haleakala
May 9, 1987	04:27:15	341.479	0.084	53.998	200.431	−0.04549	0.18223	MLRS
May 9, 1987	09:11:16	343.184	0.286	53.742	200.368	−0.19244	0.08465	Haleakala
May 10, 1987	04:54:11	343.459	0.101	52.672	200.107	−0.02686	0.10761	MLRS
Jan. 9, 1988	14:34:02	342.844	0.088	−7.259	420.476	0.01294	−0.00569	Haleakala
Oct. 1, 1988	13:02:10	19.006	0.121	9.764	129.043	0.26353	−0.11592	Haleakala
Oct. 2, 1988	13:55:35	18.314	0.093	6.340	129.105	0.27412	−0.12058	Haleakala

^a MLRS = McDonald Laser Ranging System.

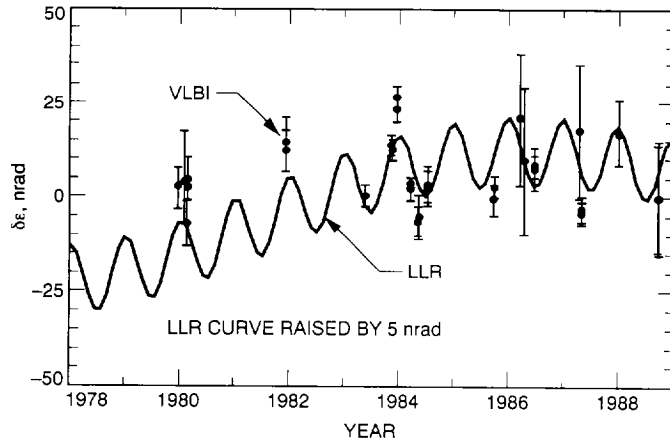


Fig. 1. Comparison of the nutation correction $\delta\epsilon$ for VLBI and LLR.

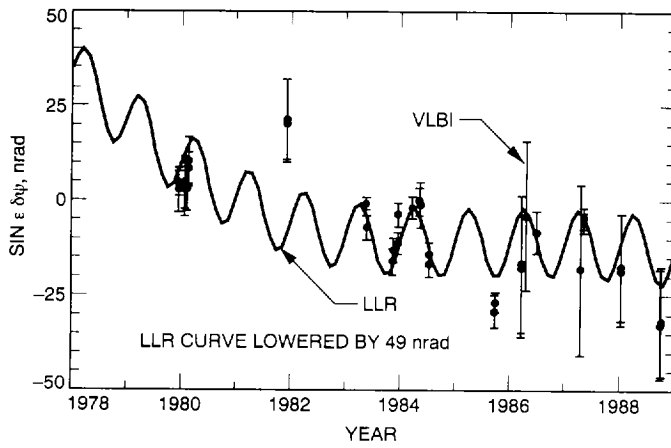


Fig. 2. Comparison of nutation correction $\delta\psi \sin \epsilon$ for VLBI and LLR.

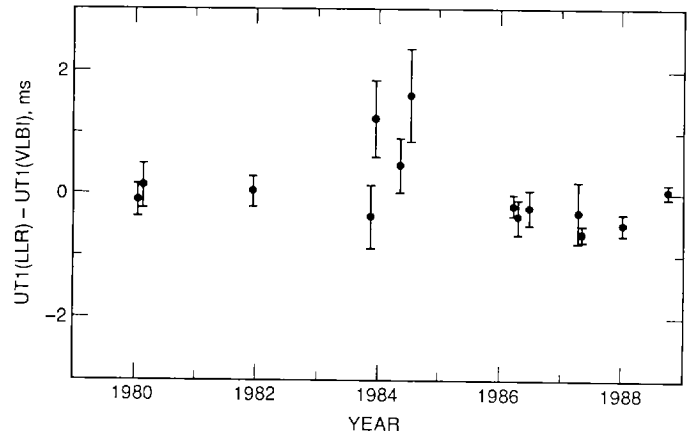


Fig. 3. Offset between the VLBI and LLR UT1 series.